Transient NMRON studies of dilute ^{54}Mn in single-crystal Fe

1994 J. Phys.: Condens. Matter 6 7109

(http://iopscience.iop.org/0953-8984/6/35/019)

J. Phys.: Condens. Matter 6 (1994) 7109–7115. Printed in the UK

Transient NMRON studies of dilute ^{54}Mn in single-crystal Fe

N Yazidjoglou, W D Hutchison and G A Stewart

Department of Physics, University College, The University of New South Wales, Australian Defence Force Academy, Campbell, ACT 2600, Australia

Received 29 March 1994

Abstract. The sign, mode magnitude, and distribution of the electric quadrupole interaction (EQI) in single-crystal ^{54}MnFe have been examined along an easy (100) direction for the first time using transient NMR on oriented nuclei (NMRON) techniques. Single-passage experiments yielded the sign of the EQI as being negative, and the modulated adiabatic passage on oriented nuclei (MAPON) technique yielded a mode magnitude and distribution for the EQI of $P/h = -4.4(4)$ kHz and $\Delta P/h = 4.0(5)$ kHz respectively. The resulting mode electric field gradient is $V_{zz} = -1.11(10) \times 10^{19}$ V m^{-2}.

1. Introduction

The present investigation continues a program of study into impurity electric quadrupole interactions (EQIs) in single-crystal hosts of crystallographically cubic iron and nickel. In earlier work (Chaplin *et al* 1988, Yazidjoglou *et al* 1990), mode values and distributions of EQIs for ^{125}SbFe, ^{125}SbNi and ^{54}MnNi single crystals along both easy and hard crystal axes were determined using modulated adiabatic passage on oriented nuclei (MAPON) spectroscopy (Callaghan *et al* 1988, Back *et al* 1988). The ^{54}MnFe system has thus been selected to allow cross-host and cross-impurity comparisons with the above-mentioned results.

MnFe specimens suitable for NMR on oriented nuclei (NMRON) are known to be difficult to prepare via diffusion techniques. This is evidenced in the literature by the use of recoil implantation (Hagn *et al* 1982) and nuclear reaction methods (Eder *et al* 1985) for the preparation of ^{52}MnFe. To the authors' knowledge, the only NMRON study of the ^{54}MnFe system was on a thermally prepared sample (Templeton and Shirley 1967) which yielded less than the full gamma ray anisotropy. Against this background, three diffused ^{54}MnFe single-crystal specimens of varying gamma ray anisotropies have been prepared and their hyperfine field distributions investigated. The first transient NMRON measurements on this system are reported for one of these specimens.

2. Experimental details

All three single-crystal ^{54}MnFe specimens were prepared by diffusing carrier-free ^{54}Mn activity into a 4 mm diameter region of the (110) surface of 1 mm thick, 6 mm diameter, Fe single crystals. Prior to diffusion, the surfaces were mechanically polished down to 0.05 μm with alumina paste. The diffusion involved annealing under an atmosphere of 50% hydrogen and 50% argon at 600 °C for 1.5 hours, after which the temperature was

0953-8984/94/357109+07$19.50

ramped to 850 °C and held for 15 minutes before cooling to room temperature over a 4.5 hour period.

Sample 1 retained 144 μCi of diffused ^{54}Mn activity after excess activity had been wiped from the surface with ethanol and lightly etched with 0.5 M HNO_3. For the diffusion conditions stated above, Ficks' laws give a root mean square diffusion depth of x_{RMS} = 2.5 μm, assuming the diffusion constant $D_0 = 0.35 \times 10^{-4}$ m^2 s^{-1} and activation energy Q = 219.8 kJ mol^{-1} (Nohara and Hirano 1970). The corresponding average ^{54}Mn concentration (given the specific activity, 245.84 mCi per mg of Mn as quoted by the supplier) is therefore 0.24 at.%.

Sample 2 was prepared from sample 1 by using 0.2 M HNO_3 (without unsoldering the sample from the cold finger) to etch away further activity. This left ~30 μCi of activity corresponding to an average ^{54}Mn concentration of 0.05 at.%.

Sample 3 was prepared by diffusing ^{54}Mn activity into a second Fe single crystal. The ~10 μCi of activity remaining after a light etch with 0.1 M HNO_3 corresponded to an average ^{54}Mn concentration of 0.02 at.%.

The samples were mounted on the copper cold finger of a dilution refrigerator with the external applied field B_{app}, and the γ-detection directed along the surface ⟨100⟩ direction as previously identified by Laue back diffraction. A pair of 12 mm diameter loops of copper wire generated the radio frequency (RF) field perpendicular to the applied field and parallel to the sample surface. Base working temperatures of ~8 mK were achieved for all NMRON measurements. The ^{54}Mn decay scheme has a single gamma ray transition at 835 keV. This peak was monitored with pulse height analysis during the continuous wave (CW) experiments, while for the pulsed frequency-modulated (FM), single-passage and MAPON experiments this line's integrated count rate was monitored using single channel analysers. All the RF power levels specified for CW experiments are source powers in dB_m while, for the transient techniques, envelope peak to peak voltages (V_{pp}) were measured into an external 50 Ω load.

3. Results

The gamma-detected 'magnetization' curves for samples 1 and 3 are shown in figure 1. Since specimen 2 was obtained by *in situ* etching of activity from sample 1, it was assumed that the form of the 'magnetization' curve for sample 2 will be identical to that for sample 1. Although sample 1 provided the greatest count rate, it realized approximately 40% of the expected gamma ray anisotropy ($1 - W(0°)$). By comparison, the lower activity samples 2 and 3 realized approximately 70% of the expected anisotropy. A slight misalignment of the ⟨100⟩ easy direction, with respect to the applied field direction, is responsible for the less than full magnetic saturation at zero field for specimen 3. Selected pulsed FM and CW resonances are shown in figure 2(a) (B_{app} = 1.64 T) and figure 2(b) (B_{app} = 0.0 T) respectively. Each of the resonances was constructed from multiple passes wherein the frequency was stepped through the line with a sequence of FM-on counting time, followed by a wait period, then an FM-off counting time. Table 1 summarizes the centre frequencies and resonance linewidths, Γ_{FWHM}, for all CW and pulsed FM experiments. The experimental errors quoted reflect only those uncertainties resulting from the resonance line fits. Figure 3 enables a visual comparison of the field-shifted centre frequencies for the three samples.

Single-frequency sweeps through the resonance (single passages) were performed on sample 1 both to determine the sign of the EQI and to select appropriate RF levels and sweep conditions for subsequent MAPON measurements. Two sets of single-passage measurements

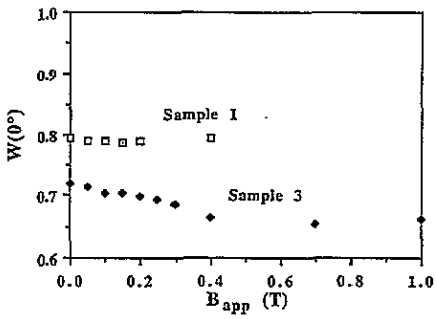

Figure 1. Gamma-detected 'magnetization' curves of ^{54}MnFe (B_{app} ∥ ⟨100⟩) determined via radiative detection of the 835 keV gamma line for samples 1 and 3.

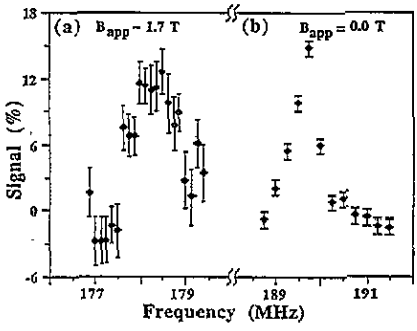

Figure 2. Selected ^{54}MnFe resonances for B_{app} ∥ ⟨100⟩. (a) Pulsed FM resonance for sample 2 at B_{app} = 1.64 T with an FM amplitude of ± 400 kHz, 400 Hz triangular modulation and a 10 ms RF pulse of amplitude V_{RF} = 81 V_{pp}. (b) CW NMRON resonance for sample 1 at B_{app} = 0.0 T with an FM amplitude of ± 125 kHz, triangular modulation frequency of 200 Hz and V_{RF} = 0 dB_m.

Table 1. Summary of lineshape parameters for CW and pulsed FM NMRON resonance spectra.

Sample	B_{app} (T)	Mode	Centre Frequency (MHz)	Γ_{FWHM} (MHz)
1	0.00	CW	189.67(2)	0.62
2	0.34	CW	189.37(4)	0.74
2	0.49	CW	188.02(6)	0.87
2	0.63	CW	186.73(8)	1.00
2	0.77	CW	185.59(12)	1.39
2	0.92	CW	184.37(8)	1.13
2	1.64	Pulsed	178.37(4)	0.94
3	0.00	CW	189.76(3)	0.62
3	0.30	CW	189.71(3)	0.91
3	0.44	CW	188.43(9)	0.67
3	0.59	CW	187.15(7)	0.78

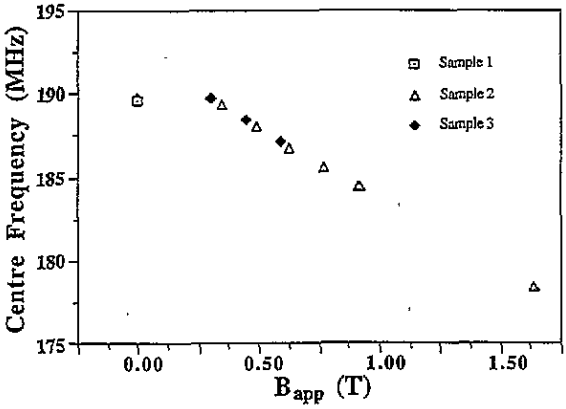

Figure 3. Centre resonance frequency as a function of applied field for each of the three ^{54}MnFe samples investigated.

(where a sweep up and sweep down constitute a set) recorded are shown in figure 4.

The first set (figure 4(a)) was recorded with $V_{RF} = 4.8\ V_{pp}$ and a 500 ms/channel dwell time. A corresponding 'off resonance' measurement revealed that approximately 15% of the available anisotropy was destroyed via non-resonant heating. The second set (figure 4(b)) was recorded with a smaller RF level, $V_{RF} = 4.0\ V_{pp}$ and a 200 ms/channel dwell time. Here the non-resonant heating was negligible and hence this set represents a pure resonant signal. Irrespective of the influence of the off-resonant heating, and despite the relative weakness of the sweep asymmetry, both sets of results correspond to a nett negative EQI. This is deduced on the basis of the slower rise to maximum signal immediately post passage for the sweep-down data, producing a more rounded initial response, and the larger (and faster) peak destruction of the sweep-up data. The slower rise to maximum signal is indicative of the RF entering the most populated quadrupolar split sub-levels first, and *vice versa* for the faster-rising signal. Further single-passage experiments were performed on the less active sample 3 (not shown). The sign of the EQI was again deduced to be negative with a similar degree of weak sweep asymmetry to that present in the single-passage NMRON relaxation curves of figure 4.

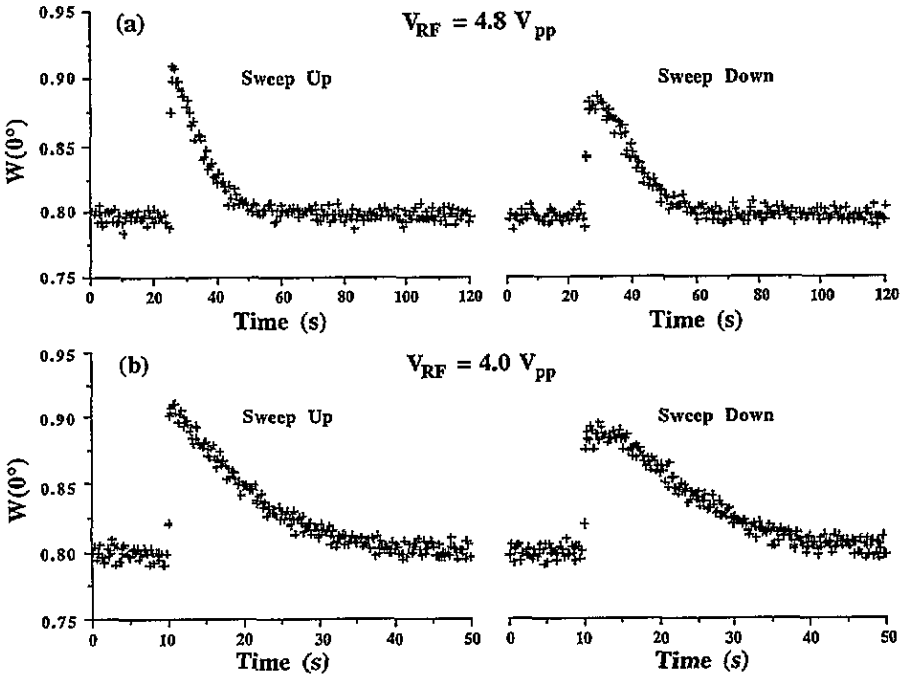

Figure 4. Single-passage NMRON relaxation curves for ^{54}MnFe ⟨100⟩ (sample 1) in zero field with a 147 ms sweep through 2 MHz centred on 189.7 MHz for (a) $V_{RF} = 4.8\ V_{pp}$ and a dwell time of 500 ms/channel and (b) $V_{RF} = 4.0\ V_{pp}$ and a dwell time of 200 ms/channel.

The plot of MAPON signal versus modulation frequency for the ⟨100⟩ direction of sample 1 is shown in figure 5(a). The parameters for this experiment were $B_{app} = 0$ T, $V_{RF} = 5.0V_{pp}$, sweep time = 147 ms (sweep up), and a sweep width of 2 MHz centred on 189.7 MHz. This data set does not show a clear signal transition or break point as the modulation frequency is increased, and shows considerable scatter on the high-frequency side. However, the differential MAPON spectrum as presented in figure 5(b) indicates a clear EQI mode value of $P/h = (3eQV_{zz})/h(4I(2I-1)' = -4.4(4)$ kHz with a FWHM of $\Delta P/h$

= 4.0(5) kHz. Although MAPON experiments were performed on sample 2, the reduced count rate (× 0.2 compared to sample 1) prevented the determination of a mode EQI value. MAPON experiments were not attempted on the even less active sample 3.

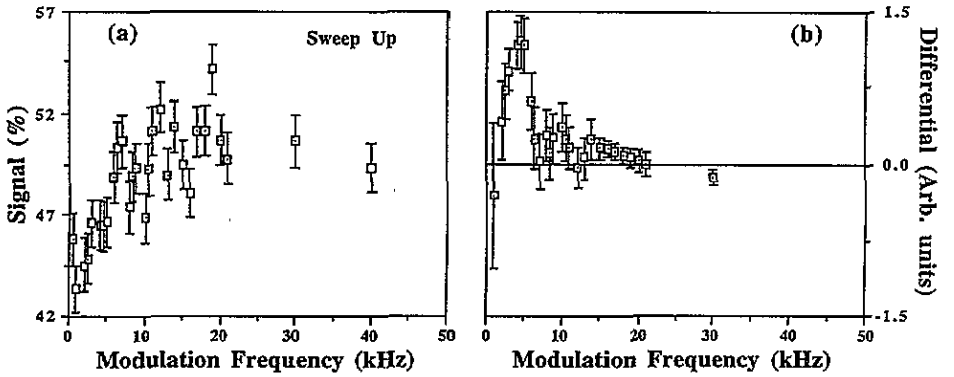

Figure 5. MAPON results for ^{54}MnFe (100) (sample 1) in zero field with a 147 ms sweep up through 2 MHz centred on 189.7 MHz and $V_{RF} = 5.0V_{pp}$. (a) The raw data and (b) the corresponding differential spectrum.

4. Discussion and conclusion

The present work confirms that it is difficult to prepare full gamma anisotropy NMRON specimens of ^{54}MnFe by thermal diffusion. Based on a simple model in which only those impurity nuclei in good substitutional sites experience a non-zero hyperfine field (namely the **full** hyperfine field), the fraction of nuclei in good sites is equivalent to the achieved fraction of full gamma-ray anisotropy. In the present work, the fractions of impurity nuclei in good sites are estimated to be approximately 40%, 70% and 70% for samples 1, 2 and 3 respectively. However, as expected for a site selective technique such as NMRON, the position and width of the resonances were observed to be independent of the achieved percentage of full gamma-ray anisotropy.

To the authors' knowledge, the only ^{54}MnFe reported to be suitable for nuclear orientation (and therefore assumed to show full gamma-ray anisotropy) was a low-count-rate specimen (thermometer) prepared by fast-neutron irradiation of a pure iron foil (Van Rijswijk *et al* 1988). The earlier CW NMRON results of Templeton and Shirley (1967) and the thermally cycled NO investigations of spin–lattice relaxation by Boysen *et al* (1984) were both reported for specimens which exhibited less than 70% of the expected gamma-ray anisotropy. In line with the above observations, the zero-field centre frequencies of samples 1 and 3 (189.67(2) MHz and 189.76(3) MHz respectively) are in excellent agreement with the result of 189.9(3) MHz reported by Templeton and Shirley (1967). Furthermore, although the impurity concentration of sample 1 (0.24 at.%) is approaching the point where one might expect concentration broadening or low/high-frequency tailing (Chaplin *et al* 1993), the more dilute sample 3 (0.02 at.%) shows a similar resonance line width in zero field (table 1). This suggests concentration effects (either homogeneous or local) are an insignificant contribution to the line broadening in sample 1.

This is supported further by the MAPON-determined EQI distribution, which provides a sensitive probe of the local environment, specifically the presence of neighbouring impurities

which would be expected to exert a dramatic influence on the local electric field gradient (EFG). The EQI distribution, $\Delta P/h$ for ^{54}MnFe sample 1, is observed to be relatively narrow, and indeed remarkably similar to that reported for ^{54}MnNi (table 2). The mode EQI value of $P/h = -4.4(4)$ kHz is also remarkably similar in magnitude to the ^{54}MnNi mode EQI (but of opposite sign). Assuming a ^{54}Mn quadrupole moment of $Q = +0.33(4)$ b (Raghavan 1989), the mode EQI value determined from this work corresponds to an EFG of $V_{zz} = -1.11(10) \times 10^{19}$ V m^{-2} at the ^{54}Mn site (z aligned with the easy ⟨100⟩ direction).

Table 2. Comparison of EQI mode value, P/h, and FWHM distribution value, $\Delta P/h$, for host easy-magnetization directions.

	Ni ⟨111⟩		Fe ⟨100⟩	
Impurity	$\frac{\bar{P}}{h}$ (kHz)	$\frac{\Delta P}{h}$ (kHz)	$\frac{\bar{P}}{h}$ (kHz)	$\frac{\Delta P}{h}$ (kHz)
^{54}Mn	+ 3.5(0.5)[a]	4.0(0.5)	− 4.4(0.4)[b]	4.0(0.5)
^{58}Co			+23.0(3.0)[c]	11.0(1.0)
^{60}Co			+ 4.5(1.0)[c]	7.5(0.5)
^{125}Sb	−20.0(4.0)[a]	50.0(5.0)	− 7.0(0.8)[a]	10.0(1.0)

[a] Chaplin *et al* (1988), Yazidjoglou *et al* (1990).
[b] *This work.*
[c] Back (1988), Back *et al* (1988).

Table 2 summarizes the easy-axis-mode EQI values determined for ^{58}Co, ^{60}Co, ^{125}Sb and ^{54}Mn in iron hosts, and ^{125}Sb and ^{54}Mn in nickel hosts. Whereas the quadrupole moments of ^{54}Mn, ^{58}Co and ^{60}Co are all positive, neither the sign nor the magnitude of the ^{125}Sb quadrupole moment is known. Hence not all EQIs can be reduced to their more fundamental EFG values. Despite this, the negative sign of the ^{54}MnFe EQI when compared to the positive sign of the ^{54}MnNi and CoFe systems clearly indicates that the dominant source of EFGs for the light impurities cannot be due to host magnetostriction. This highlights the need to consider the host–impurity combinations as a whole, rather than search for trends within like hosts or like impurities.

A striking feature of table 2 is the broader distribution of the ^{125}SbNi EQI, even if the nuclear-parameter-free figure of merit, $F = |\bar{P}|/\Delta P$ (as employed by Hutchison *et al* 1991) is considered. The situation with ^{125}SbNi is further complicated by the directional dependence of the EQI (not included in table 2). Whereas the sign of the EQI is the same along the hard and easy axes of ^{54}MnNi, ^{125}SbFe (Chaplin *et al* 1988) and the CoFe systems (Back 1988, Back *et al* 1988), it is found to reverse (negative for ⟨111⟩, positive for ⟨100⟩) for ^{125}SbNi (Yazidjoglou *et al* 1990). This seemingly anomalous behaviour of the ^{125}SbNi system will be further investigated in the near future.

New ^{58}CoNi and ^{60}CoNi EQI data currently being analysed will extend and complement the database available for cross comparison as presented in table 2. Future work on ^{54}MnFe will address the sample preparation problem by attempting an (n, p) nuclear reaction on enriched ^{54}Fe or a (d, α) nuclear reaction on ^{56}Fe. In addition, EQI determinations will be conducted for the applied field directed along the hard ⟨111⟩ axis of ^{54}MnFe, and CW and pulsed NMRON resonance line investigations to applied fields of up to 8 T will allow the Knight shift to be determined.

Acknowledgments

The authors wish to acknowledge Associate Professor D H Chaplin for his valuable

discussions and careful reading of the manuscript. This project was supported by a grant from the Australian Research Council.

References

Back P J 1988 *Hyperfine Interact.* **43** 211
Back P J, Chaplin D H and Callaghan P T 1988 *Phys. Rev.* B **37** 4911
Boysen J, Brewer W D, Bures K D, Kettschau A, Klein E, Kopp M and Wilson G V H 1984 *J. Magn. Magn. Mater.* **43** 267
Callaghan P T, Back P J and Chaplin D H 1988 *Phys. Rev.* B **37** 4900
Chaplin D H, Huang X, Hutchison W D, Stewart G A and Yazidjoglou N 1993 *Hyperfine Interact.* **80** 1263
Chaplin D H, Hutchison W D, Kopp M and Yazidjoglou N 1988 *Hyperfine Interact.* **43** 241
Eder R, Hagn E and Zech E 1985 *Phys. Rev.* C **32** 1707
Hagn E, Zech E and Eska G 1982 *J. Phys. F: Met. Phys.* **12** 1475
Hutchison W D, Edge A V J, Yazidjoglou N and Chaplin D H 1991 *Phys. Rev. Lett.* **67** 3436
Nohara K and Hirano K 1970 *Proc. Int. Conf. on Science and Technology of Iron and Steel (Tokyo, 1970)*
Raghavan P 1989 *At. Data Nucl. Data Tables* **42** 189
Templeton J E and Shirley D A 1967 *Phys. Rev. Lett.* **18** 240
Van Rijswijk W, van der Rande H S, Jilderda A A and Huiskamp W J 1988 *Hyperfine Interact.* **39** 23
Yazidjoglou N, Hutchison W D and Chaplin D H 1990 *Hyperfine Interact.* **61** 1419